

Supplemental Fig. S1

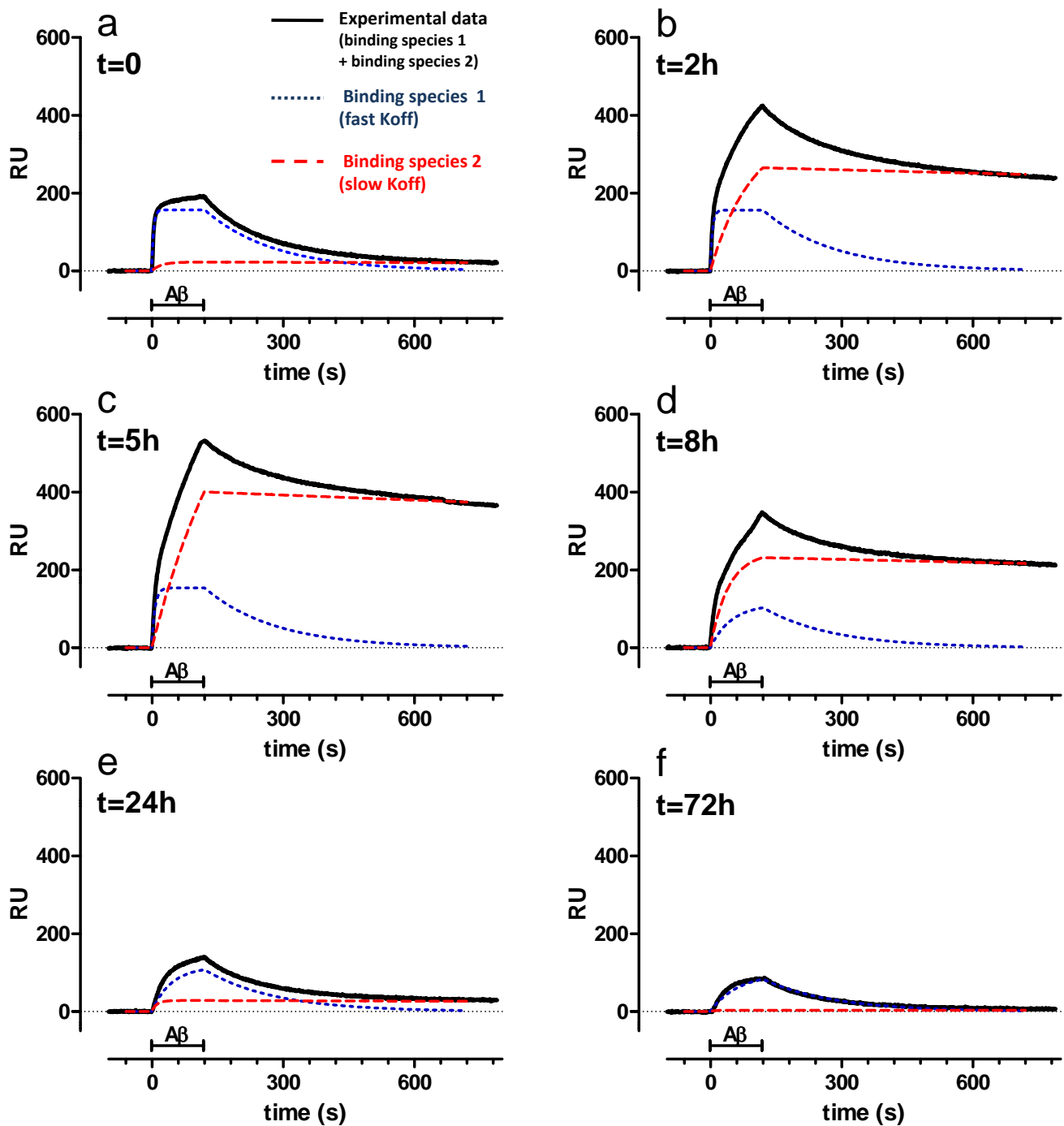
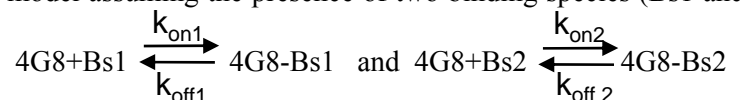


Fig. S1 SPR studies.

Synthetic A β_{1-42} (100 μ M) was incubated at 25°C and sampled at different times (from 0-72h), diluted to 1 μ M in PBS and injected over immobilized 4G8 for 2 min (bar), followed by 11 min dissociation. Black curves shows the experimental sensorgrams (time course of the SPR signal expressed in resonance units, RU). All these curves were fitted simultaneously using a model assuming the presence of two binding species (Bs1 and Bs2) and the following reaction equations :



In particular we imposed that k_{off1} and k_{off2} were the same for all the sensorgrams. According to the binding parameters, the curves corresponding to the fast-dissociating binding species ($6.3 \times 10^{-3} \text{ s}^{-1}$, blue pointed lines) and the slow-dissociating binding species ($1.1 \times 10^{-4} \text{ s}^{-1}$, red dotted lines) were obtained.

Supplemental Fig. S2

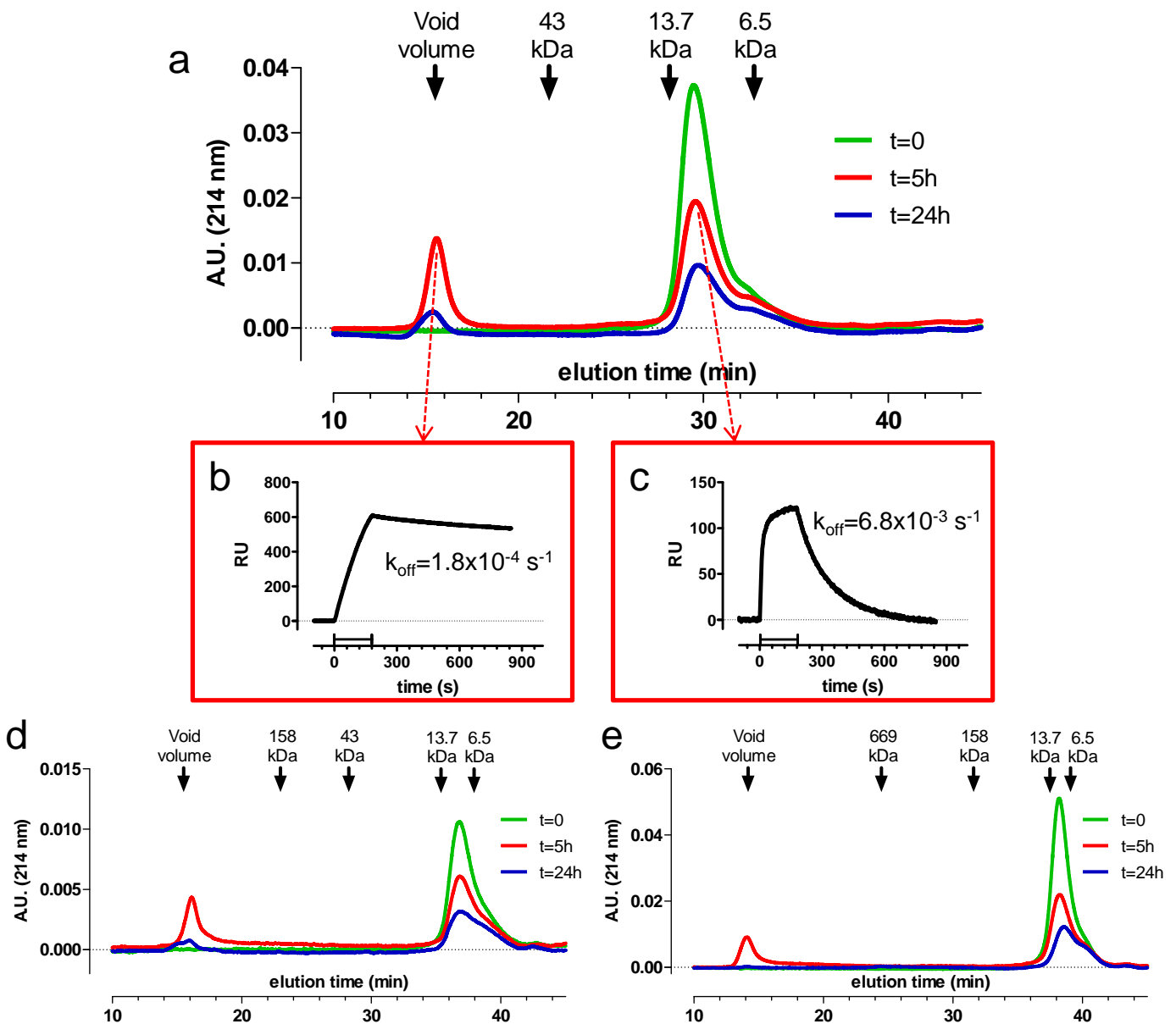


Fig. S2 Characterization of the aggregation of synthetic $A\beta_{1-42}$ at different incubation times by size exclusion chromatography.

Synthetic $A\beta_{1-42}$ (100 μM) was incubated at 25°C, sampled at different times (0, 5 and 24h), and diluted to 10 μM . a) Size-exclusion chromatography. At $t=0$, $A\beta_{1-42}$ eluted as a single peak at time corresponding to monomeric species (green trace). At 5h, another peak appeared in the void volume, indicating a soluble, high-MW species (red trace). The peak in the void volume was much smaller at $t=24\text{h}$ (blue trace). Black arrows indicate the elution times of standard proteins: aprotinin (6.5 kDa), ribonuclease-A (13.7 kDa), ovalbumin (43 kDa). Void volume was measured with blu-dextrane 2000 (2000 kDa).

b-c) Fractions collected from SEC analysis in correspondence of the two main peaks at $t=5\text{h}$ (red arrows) were injected over immobilized 4G8. Analysis of the sensorgrams indicated a mono-exponential dissociation phase with the k_{off} values indicated.

d-e) Size-exclusion chromatography of synthetic $A\beta_{1-42}$ at different incubation times using S200 and S6 columns, respectively. Black arrows indicate the elution times of standard proteins: aprotinin (6.5 kDa), ribonuclease-A (13.7 kDa), ovalbumin (43 kDa), aldolase (158 kDa), tyroglobulin (669 kDa). Void volume was measured with blu-dextrane 2000 (2000 kDa).

Supplemental Fig. S3

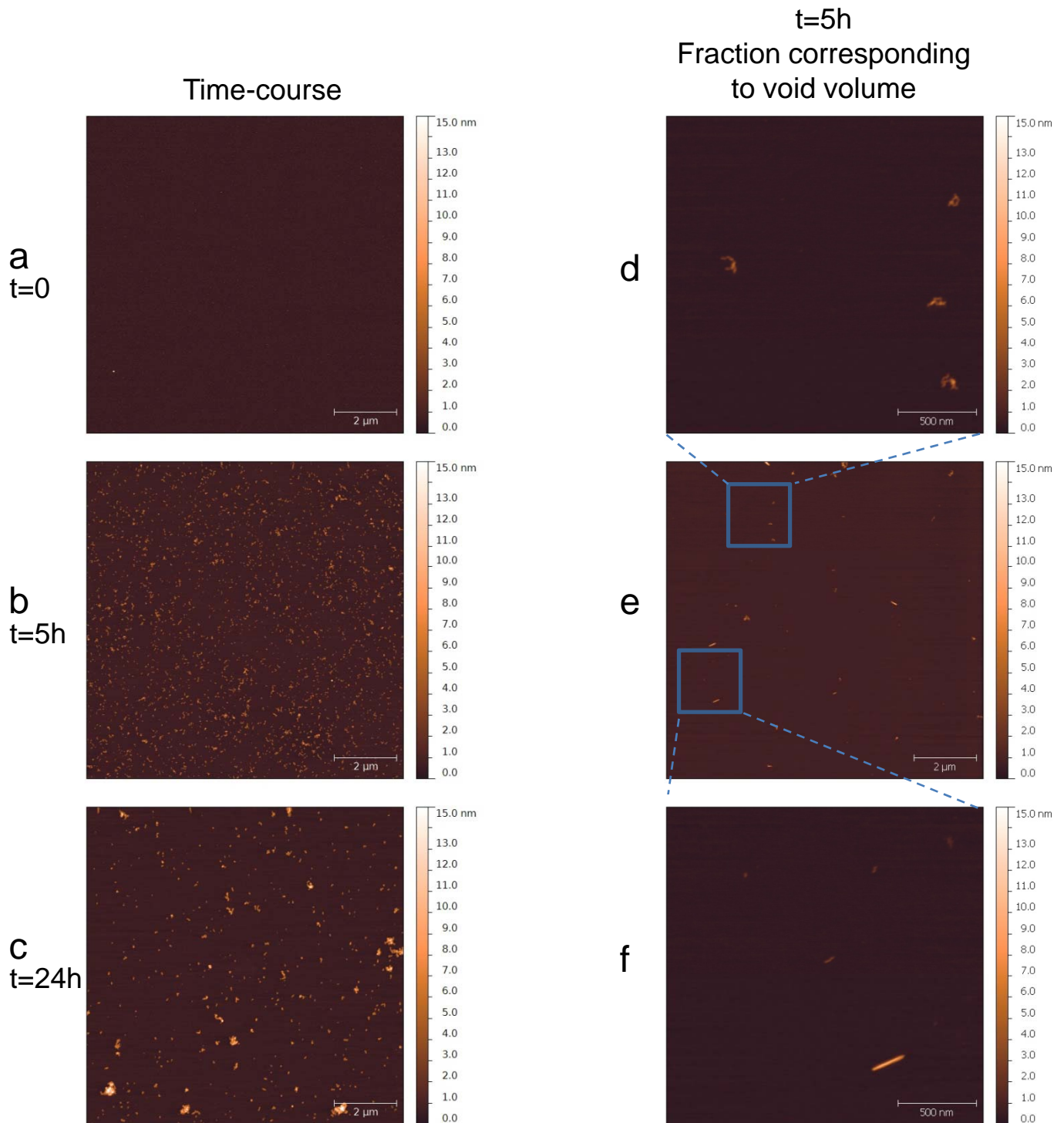


Fig. S3 Atomic force microscopy analysis.

a-c) Synthetic A β_{1-42} (100 μ M) was incubated at 25°C and sampled at different times (0, 5 and 24h), diluted to 10 μ M and left to adsorb on freshly cleaved mica.

d-f) Synthetic A β_{1-42} (100 μ M) was incubated at 25°C for 5 hours, diluted to 10 μ M and injected into SEC column (see Fig. S2c). Void volume was collected and left to adsorb on freshly cleaved mica. Panels d,f show enlargements of panel e. The lower amount of species in panel e in comparison to panel b is due to dilution of the samples during the elution in the SEC column.

Supplemental Fig. S4

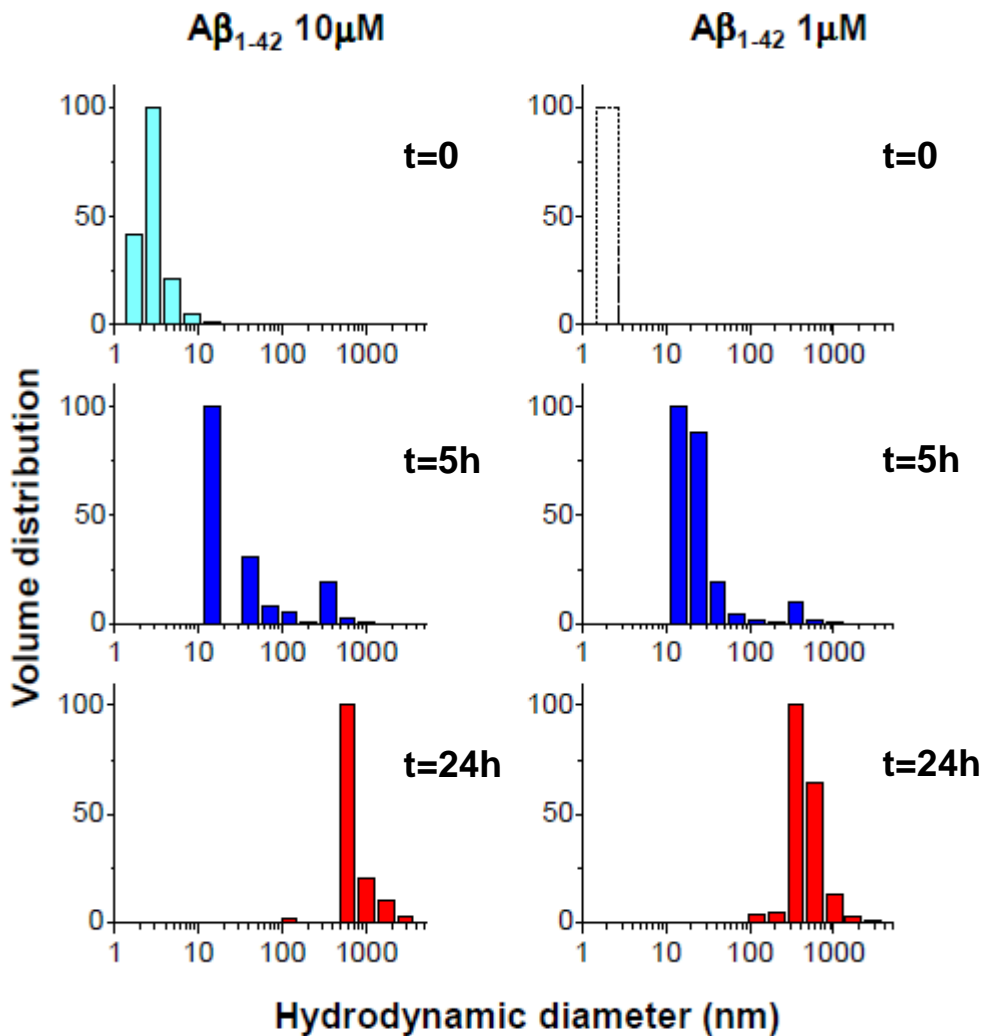


Fig. S4 Dynamic laser light scattering analysis of $A\beta_{1-42}$ particle size distribution.

Synthetic $A\beta_{1-42}$ ($100\mu\text{M}$) was incubated at 25°C , sampled at different times (0, 5 and 24h) and diluted to 1 or $10\mu\text{M}$ for analysis. The relative volume distributions have been assessed from the intensity correlation function by CONTIN method and are shown as percent of the most present specie. At $t=0$ the scattered intensity associated to very low-MW species was not enough to provide a precise size distribution, although the hydrodynamic diameter of these species is definitely below 10 nm. At $t=5\text{h}$, the size distribution was shifted to higher hydrodynamic dimensions, with a peak around 15 nm. At 24h the aggregation process leads to still soluble high-MW species with an hydrodynamic diameter in the range of 500 nm.

Supplemental Fig. S5

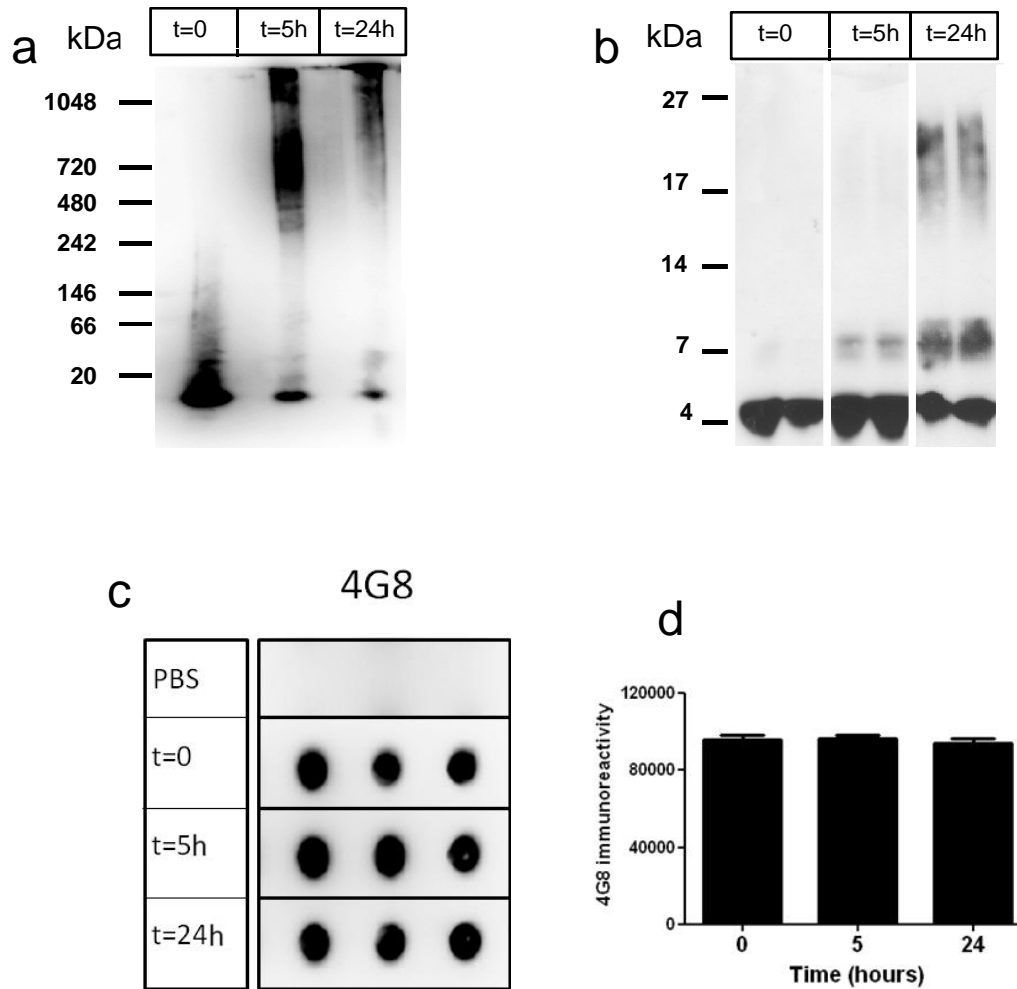


Fig. S5 Characterization of the aggregation of synthetic $A\beta_{1-42}$ at different incubation times.

Synthetic $A\beta_{1-42}$ (100 μ M) was incubated at 25°C, sampled at different times (0, 5 and 24h), diluted to 10 μ M in PBS and then analyzed by:

- Native gel electrophoresis and Western blot analysis using 4G8 antibody. Equal amount of peptide (675 ng) was loaded in each lane;
- SDS-PAGE and Western blot analysis using 4G8 antibody. Equal amount of peptide (675 ng) was loaded in each lane.
- Dot-blot analysis using 4G8. Equal amounts of peptide (50 ng) was spotted in each dot. Vehicle (PBS) was spotted as negative control.
- Quantification of the 4G8-immunoreactive dots. The mean density of the $A\beta$ -reactive spots was analyzed using Quantity One software (Bio-rad, USA). Data are the means \pm SD (N=3).

Supplemental Fig. S6

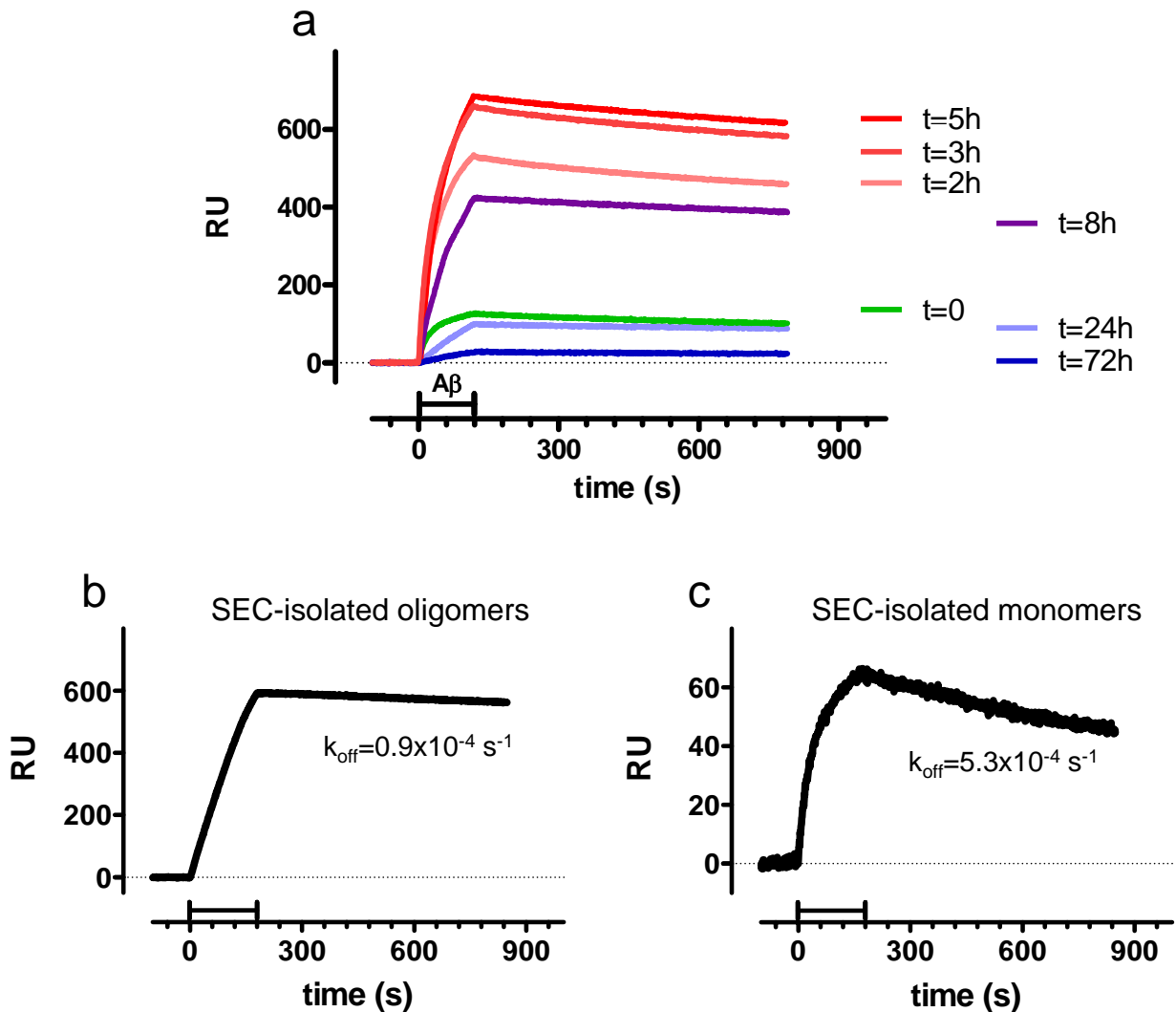


Fig. S6 SPR studies with 6E10.

(a) Synthetic Aβ₁₋₄₂ (100 μM) was incubated at 25°C and samples were taken at different times (from 0 to 72h), diluted to 1 μM in PBS and injected over immobilized 6E10 for 2 min (bar), followed by 11 min dissociation. All the sensorgrams could be well fitted by the simplest 1:1 Langmuir equation.

The fitting of the sensorgram obtained at t=0 (concentration of Aβ monomers 1 μM), indicated the following binding constants: $k_{on} : 3.8 \times 10^4 \text{ M}^{-1} \text{ s}^{-1}$; $k_{off} : 3.1 \times 10^{-4} \text{ s}^{-1}$, $K_D : 8 \text{ nM}$. Thus, 6E10 binds monomer with a K_{off} twenty-fold slower than that of 4G8. The qualitative time-course of SPR signal observed with 6E10 is similar to that observed with 4G8 (Fig. 1a) suggesting that 6E10 also binds the transient oligomeric species detected by 4G8. However, the k_{off} values of all these sensorgrams were not significantly different, ranging $1.3\text{-}3.1 \times 10^{-4} \text{ s}^{-1}$, indicating a similar k_{off} of 6E10 for both monomers and oligomers, and precluding the dissection of the contribution of the two species in the total binding.

(b-c). Sensorgrams obtained injecting the SEC fractions corresponding to monomers and oligomers (t=5h, see also Fig. S2c-e). The analysis of the sensorgrams indicated a mono-exponential dissociation phase with the k_{off} values indicated, confirming that the difference for monomers and oligomers is only 6-fold, i.e. much less than the difference observed with 4G8.

Supplemental Fig. S7

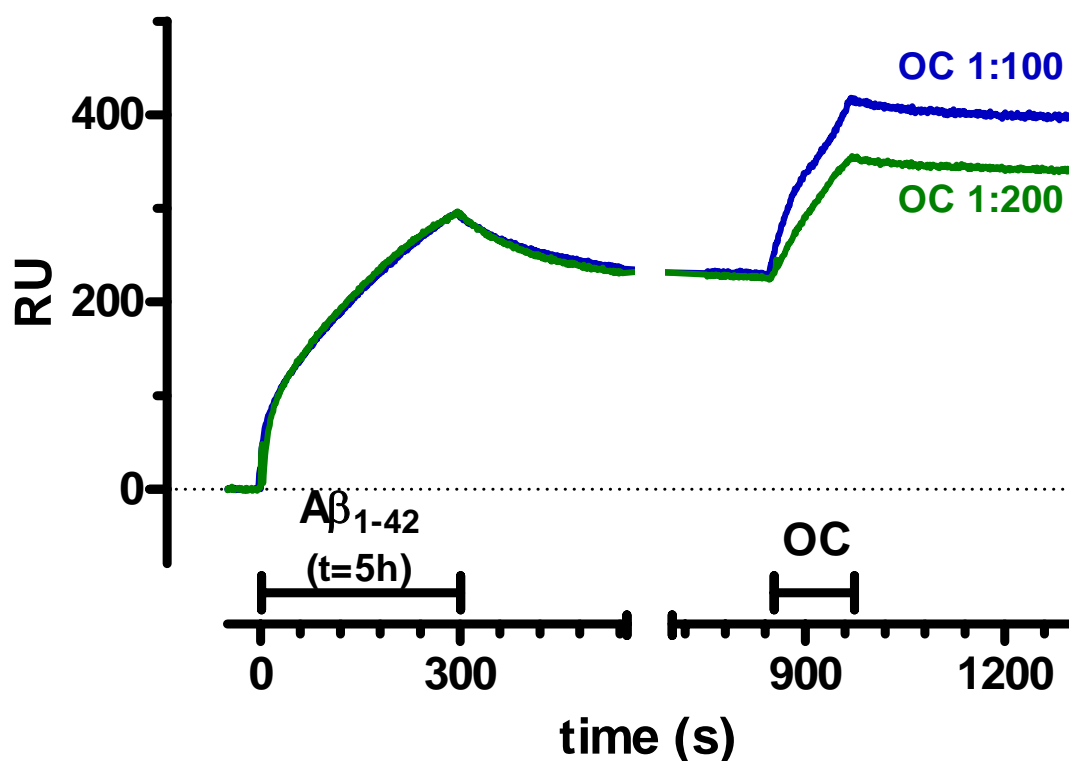


Fig. S7 SPR studies showing binding of OC to 4G8-captured $A\beta_{1-42}$ oligomers

Synthetic $A\beta_{1-42}$ (100 μM) was incubated at 25°C, sampled after 5 hours, diluted to 1 μM in PBS and injected over immobilized 4G8 for 5 min. After a dissociation phase of about 10 min, i.e. after the complete dissociation of monomeric species, only oligomeric species are stably bound to 4G8. At this point, two different concentrations of OC (1:100 and 1:200 dilutions) were injected for 2 min (bar). The sensorgrams show the specific binding of OC to oligomeric species, after correction for the small non-specific binding of OC to 4G8, determined in parallel surfaces.

Supplemental Fig. S8

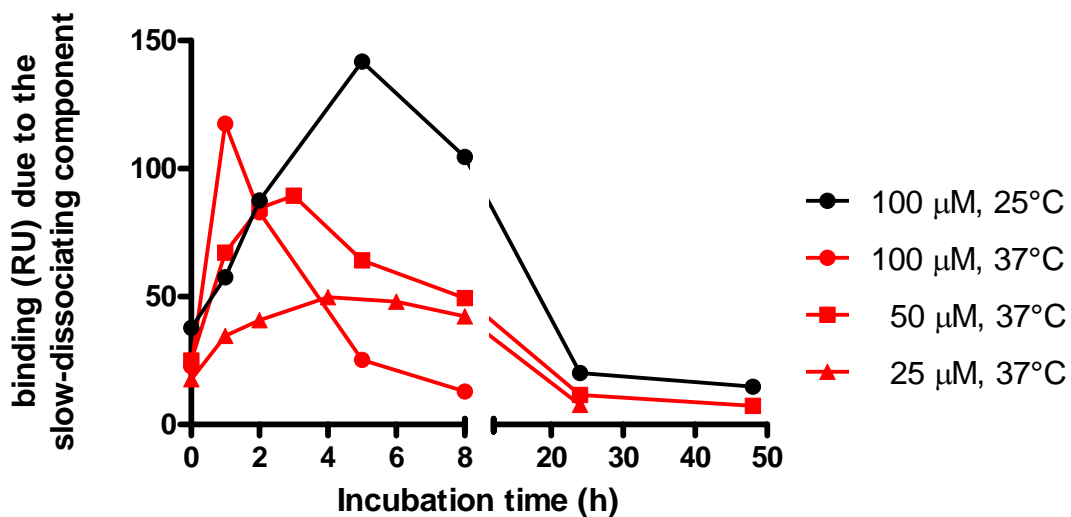


Fig. S8 Effect of $A\beta_{1-42}$ concentration and incubation temperature of on the appearance/disappearance of oligomeric species.

Synthetic $A\beta_{1-42}$ was incubated at different concentrations at 25°C or 37°C, sampled at different times, diluted to 1 μM in PBS and injected over immobilized 4G8. The sensorgrams were fitted with a model assuming the presence of two binding species with different dissociation rates (see Fig. S1). The graph reports the time-course of binding to the slowly-dissociating component, i.e. oligomeric species. These data were obtained simultaneously in the same experimental session, i.e. using the same starting solution of $A\beta_{1-42}$, incubated in parallel in the different conditions, and injected on the same sensor chip.